Chapter 7
Effect of Magnetic Field on Free and Forced Vibrations of Laminated Cylindrical Shells Containing Magnetorheological Elastomers

Gennadi Mikhasev, Ihnat Mlechka, and Svetlana Maevskaya

Abstract Free and forced vibrations of thin medium-length laminated cylindrical shells and panels assembled from elastic materials and magnetorheological elastomer (MRE) embedded between elastic layers are studied. The equivalent single layer model based on the generalized kinematic hypotheses of Timoshenko is used for the dynamic simulation of laminated shells. The full system of differential equations taking into account transverse shears, written in terms of the generalized displacements, is used to study free vibrations of long sandwich cylindrical shells with the MRE cores. To predict free and forced vibrations of medium-length sandwich cylindrical shells and panels, the simplified equations in terms of the force and displacement functions are utilized. The influence of an external magnetic field on the natural frequencies and logarithmic decrement for the MRE-based sandwich cylindrical shells is analyzed. If an applied magnetic field is nonuniform in the direction perpendicular to the shell axis, the natural modes of the medium-length cylindrical sandwich with the homogeneous MRE core are found in the form of functions decreasing far away from the generatrix at which the real part of the complex shear modulus has a local minimum. The high emphasis is placed on forced vibrations and their suppressions with the help of a magnetic field. Damping of medium-length cylindrical panels with the MRE core subjected to an external vibrational load is studied. The influence of the MRE core thickness, the level of an external magnetic field and the instant time of its application on the damping rate of forced vibrations is examined in details.

Gennadi Mikhasev · Ihnat Mlechka
Belarusian State University, 220030 Minsk, Belarus
e-mail: mikhasev@bsu.by, ignat.mlechka@gmail.com

Svetlana Maevskaya
Vitebsk State University, 210030 Vitebsk, Belarus
e-mail: svetlanamaevsckaya@ya.ru

H. Altenbach et al. (eds.), *Analysis and Modelling of Advanced Structures and Smart Systems*, Advanced Structured Materials 81,
https://doi.org/10.1007/978-981-10-6895-9_7

7.1 Introduction

Magnetorheological elastomers (MREs) belong to a new class of smart materials which due to their unique properties are gaining high interest in various areas of the structural mechanics (Gibson, 2010). MREs are composite materials consisting of a matrix (either rubbery polymer or deformed inorganic polymer) and magnetizable particles molded in this matrix. The principal mechanical characteristics of these materials are the storage and loss moduli, represented by the complex shear modulus, which are varied in a wide range when subjected to a magnetic field (Ginder, 1996; Jolly et al, 1999; Davis, 1999; Ginder et al, 2001). The MREs controllable viscoelastic properties as well as a light weight make these materials ideal to use as damping treatments or core elements in thin-walled structures experiencing an external vibrational load.

For the recent fifteen years, a considerable number of research has been carried out to observe the controllable properties and the vibration suppression capabilities of MREs embedded between elastic layers in sandwich or multilayered beams (see, among many others, Sun et al, 2003; Zhou and Wang, 2005; Howson and Zare, 2005; Zhou and Wang, 2006; Banerjee et al, 2007; Lara-Prieto et al, 2010; Korobko et al, 2012). There are much less papers on free and forced vibrations of MRE-based plates. Yeh (2013, 2014) studied the effect of different magnetic field on the modal damping and the natural frequencies for sandwich plates containing MRE cores and Aguib et al (2014); Ying et al (2014) considered forced vibrations of magnetorheological (MR) sandwich plates excited by deterministic and stochastic forces, respectively.

To the authors' best knowledge, there are only a few available papers related to the dynamic analysis of laminated shells containing cores made of a smart material with controllable elastic and rheological properties. In Yeh (2011), a three layered orthotropic cylindrical shell with an electrorheological (ER) core and outer constraining layers was considered. Introducing the complex shear modulus for the ER core and utilizing the discrete layer finite element method, the author studied the vibration and damping characteristics of the smart sandwich under different levels of applied electric fields. Mikhasev et al (2011a), applying the equivalent single layer (ESL) model for multilayered cylindrical shells, studied free vibrations of thin laminated circular cylinders with MR layers under different levels of magnetic fields. The authors concluded that an applied magnetic filed may have a significant effect on the vibration characteristics of thin MRE-based laminated cylinders. An interesting effect of distortion of natural modes in a thin medium-length cylindrical sandwich containing a polarized MRE core has been captured in Mikhasev et al (2014): an applied magnetic field may result in localization of natural modes near some lines where the real part of the reduced complex shear modulus reaches a local minimum. Recently, Mikhasev et al (2011b) studied a response of a MRE-based laminated cylindrical shell with local disturbances in their surface to an applied not stationary magnetic field. It has been shown that slowly growing magnetic fields may be used with success in order to ensure the soft suppression of running localized vibrations in thin-walled structures.

In our view, a large range of problems on free and forced vibrations of MRE-based laminated shells is not studied yet. In particular, the effect of a magnetic field on free low-frequency vibrations of medium-length cylindrical sandwich panels with MRE cores is worthy of close attention owing to a wide application of laminated panels as members of many engineering structures. Problems on the modal damping of oscillations of laminated shells with controllable MRE cores subjected to a harmonic vibrational load deserves also special attention.

A lack of detailed studies on the aforementioned and many other problems may be explained by the complexity of available models for laminated shells assembled from elastic and viscoelastic MRE laminas. In the most general terms, the known theories for multilayered shells proceed from the order of shell equations depending on a number of stacked layers (Hsu and Wang, 2005; Bolotin and Novichkov, 1980). These theories as well as available high accurate layer-wise theories (Carrera, 1999, 2002, 2003; Ferreira et al, 2011)) are rather sophisticated for practical application. The additional complexity is introduced by the coupling of the mechanical and physical (magnetic or electric) fields.

In our paper, we proceed from the idea to replace an original laminated shell containing a MRE core or layers by an equivalent single layer shell with the reduced complex moduli affected by an external magnetic field. The ESL model is expected to be more perspective for the dynamic simulation of tunable laminated thin-walled structures containing MR layers (survey articles and monographs devoted to ESL theories are, e.g., Grigolyuk and Kulikov, 1988a,b; Toorani and Lakis, 2000; Reddy, 2003; Qatu, 2004; Qatu et al, 2010). Based on the assumptions of the generalized kinematic hypothesis of Timoshenko for a whole package of a laminated shell (Grigolyuk and Kulikov, 1988b), we assume differential equations written in terms of displacements (or in terms of the force and shear functions where it is required) for the reference surface of a laminated shell as the governing equations. These equations contain coefficients depending on the complex Young's and shear moduli and the magnetic field induction as well, they being the generalization (Mikhasev et al, 2011a) of analogous equations derived in Grigolyuk and Kulikov (1988b) for elastic laminated shells. The basic purpose of the paper is to study free vibrations of sandwich cylindrical shells and panels with the MRE cores under various levels of applied external magnetic fields. The effect of a nonuniform magnetic field on the natural modes corresponding to low-frequency vibrations of a thin medium-length circular cylindrical sandwich shell containing the MRE core is also analyzed. The special attention is focused on the problem of suppression of forced vibrations in MRE panels subjected to a harmonic vibrational load under an external magnetic field.

7.2 Structure of Laminated Shell

Consider a thin laminated package in the form of a circular cylinder or panel of the length L (see Fig. 7.1). Let it consist of N isotropic or transversely isotropic layers

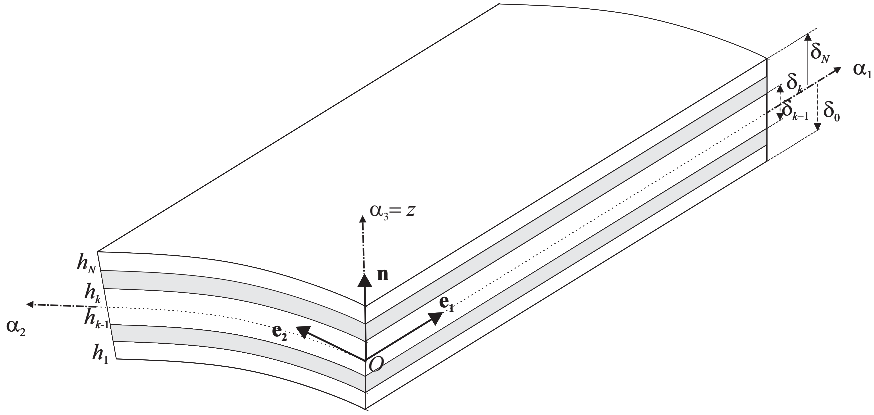

Fig. 7.1: Laminated cylindrical shell with a curvilinear coordinate system

characterized by thickness h_k, density ρ_k, Young's modulus E_k, shear modulus G_k and Poisson's ratio ν_k, where $k = 1,2,\ldots,N$, and N is an odd number. The middle surface of any fixed layer is taken as the reference surface. We introduce a local orthogonal coordinate system by means of unit vectors $\mathbf{e}_1, \mathbf{e}_2$ and $\mathbf{n} = \mathbf{e}_1 \times \mathbf{e}_2$ with an origin in the point O at the reference surface as shown in Fig. 7.1. Let α_1 and α_2 be the axial and circumferential coordinates, respectively, and $\alpha_3 = z$ is the normal coordinate. The radius of curvature of the reference surface is $R = 1/k_{22}$.

Laminas with odd numbers (numbering begins with the innermost layer) are made of an elastic material, while layers with even numbers are made of a magnetorheological elastomer (MRE) whose rheological properties depend on intensity of an applied magnetic field. For layers made of a MRE, the Young's and shear moduli, E_k, G_k, are assumed to be complex functions of the magnetic field induction B:

$$E_k = E'_k(B) + \mathrm{i}G''_k(B), \qquad G_k = G'_k(B) + \mathrm{i}G''_k(B), \tag{7.1}$$

where $\mathrm{i} = \sqrt{-1}$ is the imaginary unite. If the MRE layer is considered as an isotropic material, then

$$G_k = \frac{E_k}{2(1+\nu_k)},$$

otherwise (for a transversally isotropic layer), E_k and G_k are independent magnitudes. Here, each viscoelastic MRE layer is considered as the isotropic material with Poissons's ratio (White and Choi, 2005) $\nu_v = 0.4$ and the shear modulus $G_v = G'_v + \mathrm{i}G''_v$ specified in Korobko et al (2012). For this MRE, the dependence of the storage and loss moduli, G'_v, G''_v, on the magnetic field induction B are shown in Fig. 7.2. If an applied magnetic field is non-homogeneous, then $E_v[B(\alpha_1,\alpha_2)]$, $G_v[B(\alpha_1,\alpha_2)]$ corresponding to the MRE layers are functions of coordinates α_1, α_2.

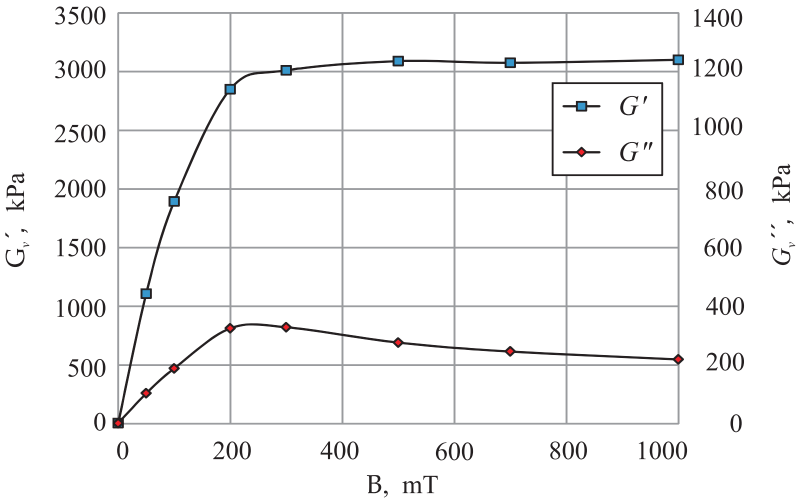

Fig. 7.2: Storage and loss moduli G'_v, G''_v (kPa) of the MRE vs. the magnetic field induction B (mT)

7.3 Basic Hypotheses

To study vibrations of multilayered shells, we will use the ESL model (Grigolyuk and Kulikov, 1988b) based on the generalized hypothesis of Timoshenko. Let $z = \delta_k$ be the coordinate of the upper bound of the k^{th} layer, u_i and w the tangential and normal displacements of the reference surface points, respectively, $u_i^{(k)}$ the tangential displacements of points of the k^{th} layer, σ_{i3} the transverse shear stresses, Θ_i the angles of rotation of the normal $\mathbf{n}$ about the vector $\mathbf{e}_i$ (see Fig. 7.1). Here $i = 1,2; k = 1,2,\ldots,N$.

Let us assume the following hypothesis (Grigolyuk and Kulikov, 1988b):

1. The distribution law of the transverse tangent stresses across the thickness of the k^{th} layer is assumed to be of the form

$$\sigma_{i3} = f_0(z)\mu_i^{(0)}(\alpha_1,\alpha_2) + f_k(z)\mu_i^{(k)}(\alpha_1,\alpha_2)\,, \tag{7.2}$$

where $f_0(z), f_k(z)$ are continuous functions introduced as follows

$$\begin{aligned} f_0(z) &= \frac{1}{h^2}(z-\delta_0)(\delta_N - z),\\ f_k(z) &= \frac{1}{h_k^2}(z-\delta_{k-1})(\delta_k - z) \end{aligned} \tag{7.3}$$

2. Normal stresses acting on the area elements parallel to the reference one are negligible with respect to other components of the stress tensor.
3. The normal deflection w does not depend on the co-ordinate z.
4. The tangential displacements are distributed across thickness of the layer package as follows:

$$u_i^{(k)}(\alpha_1,\alpha_2,z) = u_i(\alpha_1,\alpha_2) + z\Theta_i(\alpha_1,\alpha_2) + g(z)\psi_i(\alpha_1,\alpha_2) \tag{7.4}$$

where

$$g(z) = \int_0^z f_0(x)dx.$$

In Eq. (7.4), ψ_i are required parameters characterizing the transverse shears in the shell. Hypothesis (7.4) permits to describe the non-linear dependence of the tangential displacements on z; at $g \equiv 0$ it turns into the linear Timoshenko hypothesis coinciding with the classical Kirchhoff-Love hypothesis since θ_i are functions of the tangential displacements and derivatives of the normal deflection. Assumption (7.4) is called the generalized kinematic hypothesis of Timoshenko.

7.4 Governing Equations

7.4.1 Governing Equations in Terms of Stress Resultants and Couples

Using the variational principle and based on the aforementioned hypotheses, Grigoliuk and Kulikov have derived the equations in terms of the membrane stress resultants T_{ij} and the reduced stress couples $\hat{L}_{ij}$, $\hat{M}_{ij}$ (Grigolyuk and Kulikov, 1988b):

$$\begin{aligned}
&T_{1i,1} + T_{2i,2} = q_i(\alpha_1,\alpha_2,t) - \sum_{k=1}^{N}\rho_k h_k \frac{\partial^2 \hat{u}_i}{\partial t^2} = 0, \quad i = 1,2,\\
&\hat{L}_{1i,1} + \hat{L}_{2i,2} = Q_{0i}, \quad i = 1,2,\\
&\hat{M}_{11,11} + 2\hat{M}_{12,12} + \hat{M}_{22,22} - k_{22}T_{22} = q_n(\alpha_1,\alpha_2,t) - \sum_{k=1}^{N}\rho_k h_k \frac{\partial^2 w}{\partial t^2} = 0,
\end{aligned} \tag{7.5}$$

where $Z_{,i}$ designates the derivative of a function Z by α_i, t is time, q_i, q_n are the tangential and normal components of an external force, Q_{0i} is the generalized shear stress resultant. The stress resultants and couples T_{ij}, Q_{0i}, $\hat{L}_{ij}$, $\hat{M}_{ij}$ are linked with the normal, tangential and shear displacements w, u_i, ψ_i by the following equations:

$$T_{ii} = \frac{Eh}{1-\nu^2}\left[\hat{u}_{i,i} + \nu\left(\hat{u}_{j,j} + k_{22}w\right)\right], \quad T_{ij} = \frac{Eh}{2(1+\nu)}\left(\hat{u}_{i,j} + \hat{u}_{j,i}\right),$$
$$\hat{M}_{ii} = -\frac{Eh^3}{12(1-\nu^2)}\left[\eta_3(w_{,ii} + \nu w_{,jj}) - \eta_2(\psi_{i,i} + \nu\psi_{j,j})\right],$$
$$\hat{M}_{ij} = -\frac{Eh^3}{12(1+\nu)}\left[\eta_3 w_{,ij} - \frac{1}{2}\eta_2(\psi_{i,j} + \psi_{j,i})\right], \tag{7.6}$$
$$\hat{L}_{ii} = -\frac{Eh^3}{12(1-\nu^2)}\left[\eta_2(w_{,ii} + \nu w_{,jj}) - \eta_1(\psi_{i,i} + \nu\psi_{j,j})\right],$$
$$\hat{L}_{ij} = -\frac{Eh^3}{12(1+\nu)}\left[\eta_2 w_{,ij} - \frac{1}{2}\eta_1(\psi_{i,j} + \psi_{j,i})\right], \quad Q_{0i} = q_{44}\psi_i,$$

where

$$h = \sum_{k=1}^{N} h_k, \quad E = \frac{1-\nu^2}{h}\sum_{k=1}^{N}\frac{E_k h_k}{1-\nu_k^2}, \qquad \nu = \sum_{k=1}^{N}\frac{E_k h_k \nu_k}{1-\nu_k^2}\left(\sum_{k=1}^{N}\frac{E_k h_k}{1-\nu_k^2}\right)^{-1} \tag{7.7}$$

are the total thickness, reduced Young's modulus and Poisson's ratio, respectively,

$$\hat{u}_i = u_i - \frac{1}{2}hc_{13}w_{,i} - \frac{1}{2}hc_{12}\psi_i \tag{7.8}$$

is the generalized displacements, and parameters $\eta_1, \eta_2, \eta_3, c_{12}, c_{13}$ are introduced as follows:

$$\begin{gathered}
c_{12} = \sum_{k=1}^{N}\xi_k^{-1}\pi_{3k}\gamma_k, \quad c_{13} = \sum_{k=1}^{N}(\zeta_{k-1} + \zeta_k)\gamma_k, \\
\frac{1}{12}h^3\pi_{1k} = \int_{\delta_{k-1}}^{\delta_k} g^2(z)\mathrm{d}z, \quad \frac{1}{12}h^3\pi_{2k} = \int_{\delta_{k-1}}^{\delta_k} z\,g(z)\mathrm{d}z, \\
\frac{1}{2}h^2\pi_{3k} = \int_{\delta_{k-1}}^{\delta_k} g(z)\mathrm{d}z, \quad \eta_1 = \sum_{k=1}^{N}\xi_k^{-1}\pi_{1k}\gamma_k - 3c_{12}^2, \\
\eta_2 = \sum_{k=1}^{N}\xi_k^{-1}\pi_{2k}\gamma_k - 3c_{12}c_{13}, \quad \eta_3 = 4\sum_{k=1}^{N}\left(\xi_k^2 + 3\zeta_{k-1}\zeta_k\right)\gamma_k - 3c_{13}^2, \\
h\xi_k = h_k, \quad h\zeta_n = \delta_n\,(n = 0, k), \quad q_{44} = \frac{\left[\sum\limits_{k=1}^{N}\left(\lambda_k - \dfrac{\lambda_{k0}^2}{\lambda_{kk}}\right)\right]^2}{\sum\limits_{k=1}^{N}\left(\lambda_k - \frac{\lambda_{k0}^2}{\lambda_{kk}}\right)G_k^{-1}} + \sum_{k=1}^{N}\frac{\lambda_{k0}^2}{\lambda_{kk}}G_k, \\
\lambda_k = \int_{\delta_{k-1}}^{\delta_k} f_0^2(z)\mathrm{d}z, \quad \lambda_{kn} = \int_{\delta_{k-1}}^{\delta_k} f_k(z)f_n(z)\mathrm{d}z, \quad (n = 0, k).
\end{gathered} \tag{7.9}$$

In what follows, the magnitude $G = q_{44}/h$ will be called the reduced shear modulus for the laminated package. Here, the reduced moduli E, ν, G and parameters η_1, η_2, η_3 are functions of the induction B.

From all variants of boundary conditions, we consider here the simply supported edges with diaphragms. In terms of displacements, stress resultants and stress couples these conditions read:

$$w = \hat{u}_2 = \psi_2 = \hat{M}_{11} = T_{11} = \hat{L}_{11} = 0 \quad \text{at} \quad \alpha_1 = 0, L. \tag{7.10}$$

7.4.2 Governing Equations in Terms of Displacements

Let the MRE be a homogeneous and isotropic material, and an applied magnetic field is uniform. Then the substitution of Eqs. (7.11), (7.6) into Eqs. (7.5) results in the following system of differential equations:

$$\begin{aligned}
&\frac{\partial^2 \hat{u}_1}{\partial \alpha_1^2} + \frac{1-\nu}{2}\frac{\partial^2 \hat{u}_1}{\partial \alpha_2^2} + \frac{1+\nu}{2}\frac{\partial^2 \hat{u}_2}{\partial \alpha_1 \partial \alpha_2} + \nu k_{22}\frac{\partial w}{\partial \alpha_1} + \frac{\rho_0(1-\nu^2)}{E}\frac{\partial^2 \hat{u}_1}{\partial t^2} = q_1, \\
&\frac{1+\nu}{2}\frac{\partial^2 \hat{u}_1}{\partial \alpha_1 \partial \alpha_2} + \frac{1-\nu}{2}\frac{\partial^2 \hat{u}_2}{\partial \alpha_1^2} + \frac{\partial^2 \hat{u}_2}{\partial \alpha_2^2} + \frac{\partial (k_{22} w)}{\partial \alpha_2} + \frac{\rho_0(1-\nu^2)}{E}\frac{\partial^2 \hat{u}_2}{\partial t^2} = q_2, \\
&\eta_2 \frac{\partial(\triangle w)}{\partial \alpha_1} - \eta_1\left(\frac{\partial^2 \psi_1}{\partial \alpha_1^2} + \frac{1+\nu}{2}\frac{\partial^2 \psi_2}{\partial \alpha_1 \partial \alpha_2} + \frac{1-\nu}{2}\frac{\partial^2 \psi_1}{\partial \alpha_2^2}\right) + \frac{12(1-\nu^2)q_{44}}{Eh^3}\psi_1 = 0, \\
&\eta_2 \frac{\partial(\triangle w)}{\partial \alpha_2} - \eta_1\left(\frac{\partial^2 \psi_2}{\partial \alpha_2^2} + \frac{1+\nu}{2}\frac{\partial^2 \psi_1}{\partial \alpha_1 \partial \alpha_2} + \frac{1-\nu}{2}\frac{\partial^2 \psi_2}{\partial \alpha_1^2}\right) + \frac{12(1-\nu^2)q_{44}}{Eh^3}\psi_2 = 0, \\
&\frac{h^2}{12(1-\nu^2)}\triangle\left[\eta_3 \triangle w - \eta_2\left(\frac{\partial \psi_1}{\partial \alpha_1} + \frac{\partial \psi_2}{\partial \alpha_2}\right)\right] \\
&\qquad + \frac{k_{22}}{1-\nu^2}\left(\nu \frac{\partial \hat{u}_1}{\partial \alpha_1} + \frac{\partial \hat{u}_2}{\partial \alpha_2} + k_{22} w\right) + \frac{\rho_0}{E}\frac{\partial^2 w}{\partial t^2} = q_n,
\end{aligned} \tag{7.11}$$

where

$$\rho_0 = \sum_{k=1}^{N} \rho_k \xi_k$$

is the reduced density of the laminated shell.

When introducing the stress-displacement relations (7.6) into (7.10), one obtains the boundary conditions in terms of displacements:

$$
\begin{gathered}
w = \hat{u}_2 = \psi_2 = 0, \\
\eta_3\left(\frac{\partial^2 w}{\partial \alpha_1^2} + \nu\frac{\partial^2 w}{\partial \alpha_2^2}\right) - \eta_2\left(\frac{\partial \psi_1}{\partial \alpha_1} + \nu\frac{\partial \psi_2}{\partial \alpha_2}\right) = 0, \\
\frac{\partial \hat{u}_1}{\partial \alpha_1} + \nu\frac{\partial \hat{u}_2}{\partial \alpha_2} + \frac{\nu}{R w} = 0, \\
\eta_2\left(\frac{\partial^2 w}{\partial \alpha_1^2} + \nu\frac{\partial^2 w}{\partial \alpha_2^2}\right) - \eta_1\left(\frac{\partial \psi_1}{\partial \alpha_1} + \nu\frac{\partial \psi_2}{\partial \alpha_2}\right) = 0 \quad \text{at} \quad \alpha_1 = 0, L.
\end{gathered}
\tag{7.12}
$$

Equations (7.11) are sufficiently complicated for analyzing both free and forced vibrations of MRE-based cylindrical shells. However, they will be useful to study free axisymmetric vibrations of circular cylindrical shells or beam-like modes of length cylinders. To predict eigenmodes corresponding to low-frequency vibrations of thin medium-length cylindrical shells, we will apply to equations of the technical shell theory.

7.4.3 Equations of Technical Shell Theory

Let us introduce the index of variation ι of the stress-strain state as

$$
\max\{|Z_{,1}|,\ |Z_{,2}|\} \sim h_*^{-\iota} Z, \tag{7.13}
$$

where $h_* = h/R$ is the dimensional thickness which is assumed as a small parameter. We will consider here the stress state which is characterized by the index of variation $\iota = 1/2$ and the following asymptotic estimates:

$$
w \sim h_* R, \quad k_{22} \sim R^{-1}, \quad u_i \ll w. \tag{7.14}
$$

It is obvious that $\hat{u}_i \ll w$ also. Let

$$
\max\{\hat{u}_i\} \sim h_*^{\zeta_u} R, \quad \max\{\psi_i\} \sim h_*^{\zeta_\psi}, \quad G \sim h_*^{\zeta_G} E, \tag{7.15}
$$

where ζ_u, ζ_ψ are the indexes of intensity of the quantities $\hat{u}_i, \psi_i$, respectively, and $h_*^{\zeta_G}$ is the order of the reduced shear modulus G with regard to the reduced Young's modulus E. Then, analyzing the orders of all terms in Eqs. (7.11), we find

$$
\zeta_u = 3/2, \quad \zeta_\psi = 1/2, \quad \zeta_G = 1. \tag{7.16}
$$

Let $q_i = 0$ and the inertia forces in the tangential directions be very small. Then the first two equations of system (7.5) or (7.11) become homogeneous. They are identically satisfied by the following functions:

$$
T_{ij} = \delta_{ij} \triangle F - F_{,ij}, \tag{7.17}
$$

where δ_{ij} is the Kronecker delta, and F is the required stress function.

To couple the introduced stress function with the unknown displacements, we consider the strain compatibility conditions. They results in the well-known differential equation

$$\triangle^2 F - Ehk_{22}w_{,11} = 0. \tag{7.18}$$

Considering the residual equations from (7.5), Grigolyuk and Kulikov (1988b) have derived the following equations:

$$\begin{aligned} &D\left(1-\frac{\theta h^2}{\beta}\triangle\right)\triangle^2\chi - k_{22}F_{,11} = q_n - \rho_0 h\frac{\partial^2}{\partial t^2}\left(1-\frac{h^2}{\beta}\triangle\right)\chi, \\ &w = \left(1-\frac{h^2}{\beta}\triangle\right)\chi, \end{aligned} \tag{7.19}$$

where

$$\begin{aligned} D &= \frac{Eh^3\eta_3}{12(1-\nu^2)}, \\ \beta &= \frac{12(1-\nu^2)q_{44}}{Eh\eta_1} \end{aligned} \tag{7.20}$$

are the reduced bending stiffness and shear parameter, respectively.

From the third and fourth equations of (7.11), one can find the shear displacements

$$\begin{aligned} \psi_1 &= a_{,1} + \phi_{,2}, \\ \psi_2 &= a_{,2} - \phi_{,1}, \end{aligned} \tag{7.21}$$

where

$$a = -\frac{\eta_2}{\eta_1}\frac{h^2}{\beta}\triangle\chi, \tag{7.22}$$

and ϕ is the shear function which is defined from the additional equation

$$\frac{1-\nu}{2}\frac{h^2}{\beta}\triangle\phi = \phi. \tag{7.23}$$

Equation (7.23) describes the shear edge effect and should be taken into account if a simply supported edge is free of a diaphragm preventing transverse shears (Mikhasev and G., 2017). If all simply supported edges have the diaphragms, one can assume (Grigolyuk and Kulikov, 1988b) $\phi \equiv 0$. The correspondent boundary conditions in terms of functions χ, F read

$$\chi = \triangle\chi = \triangle^2\chi = F = \triangle F = 0 \quad \text{at} \quad \alpha_1 = 0, L_1. \tag{7.24}$$

If the shell is not closed in the circumferential direction, then the boundary conditions for the simply supported edges $\alpha_2 = 0, L_2$ with diaphragms are the same.

7.4.4 Error of Governing Equations

The determination of an exact error of the above equations based on the ESL model is a complicated problem. One way to estimate their error is to compare eigenvalues of some boundary-value problem on buckling or vibrations with results obtained with the help of the 3D FEM simulation. Similar comparative analysis (Mikhasev et al, 2001) has shown that accuracy of these equations is satisfactory if a shell is sufficiently thin and its vibrations occur with minor sizes of deflections or wave length. In this subsection, we aim only to give some *asymptotic* estimations of errors.

It is known that an error δ_e of the Kirchhoff-Love hypotheses has the order $\delta_e \sim h_*$. It maybe expected that accepted here the generalized Timoshenko hypotheses improves an accuracy of the governing equations and results in the error $\delta_e \sim h_*^q$, where $q \geq 1$. However, as has been shown by Gol'denveiser (1961); Koiter (1966), the index of variation ι of an expected solution may give the conclusive contribution in the estimation of an error. If $\iota < 1$, then within the framework of the Kirchhoff-Love hypotheses, this estimation is found as

$$\delta_e \sim \max\left\{h_*, h_*^{2-2\iota}\right\}.$$

For Eqs. (7.11) based on the generalized Timoshenko hypotheses, we have

$$\delta_e \sim \max\left\{h_*^q, h_*^{2-2\iota}\right\}, \tag{7.25}$$

where $q \geq 1$. The peculiarity of Eqs. (7.11) is that due to shears they have solutions with very high index of variation. So, for an elastic, isotropic and homogeneous shell with Young's and shear moduli E, G of the same asymptotic order ($E \sim G$), one obtains additional integrals which account for shears and have the index of variation $\iota = 1$. Then $\delta_e \sim 1$ and Eqs. (7.11) as well as Eqs. (7.18)-(7.23) become asymptotically incorrect. But if

$$G_r \sim h_*^{\zeta_G} E_r,$$

where $\zeta_G > 0$, then $\iota = 1 - \zeta_G/2 < 1$. Here, $E_r = \Re E$, $G_r = \Re G$ are the real parts of the complex moduli E, G for viscoelastic shells.

Now, consider Eqs. (7.18)-(7.23) which are analogous to the well-known Mushtari-Donnell-Vlasov type equations (Mushtari and Galimov, 1961; Donnell, 1976; Wlassow, 1958). They were obtained after significant simplifications which introduced the error of an order $h_*^{2\iota}$. It is seen that the error of these equations is

$$\delta_e \sim \max\left\{h_*^{2\iota}, h_*^{2-2\iota}\right\}. \tag{7.26}$$

We remind that Eqs. (7.18)-(7.23) were derived under assumptions that $\iota = 1/2$, $\zeta_G = 1$. Hence, for vibration modes with the index $\iota = 1/2$, one obtains the error $\delta_e \sim h_*$. However, Eqs. (7.18)-(7.23) can be also used to describe the *semi-momentless* dynamic stress state characterized by the index of variation $\iota = 1/4$ for a shear pliable shell with $\zeta_G \geq 1$. However, for solutions having the index of variation $\iota = 1/4$ (at $\zeta_G = 3/2$), the error increases and reaches the order $\delta_e \sim h_*^{1/2}$.

Note also that Eqs. (7.11) and Eqs. (7.18)-(7.23) as well have been derived for cases when all the reduced moduli are constant (not dependent of coordinates α_1, α_2). However, Eqs. (7.18)-(7.23) may be utilized for the analysis of low-frequency vibrations of medium-length thin laminated cylindrical shell if MRE layers are nonhomogeneous and/or an applied magnetic field is nonuniform. In Mikhasev et al (2011a) have generalized Eqs. (7.18)-(7.23) for the case when the reduced moduli E, G, ν and shear parameters η_k, β are functions of coordinates α_1, α_2 and the magnetic field induction B and time t. It has been also shown that if

$$y \sim R \frac{\partial y}{\partial \alpha_i},$$

where y is any of the functions E, G, ν, η_k, β of coordinates α_1, α_2, and $\iota = 1/4$, then the generalized equations (with variable coefficients) written in terms of functions χ, F, ϕ (Mikhasev et al, 2011a) may be substituted by the simplified Eqs. (7.18)-(7.23) derived in Grigolyuk and Kulikov (1988b), these simplified equations giving the error of an order $h_*^{1/4}$. In what follows, Eqs. (7.18)-(7.23) will be used to analyse free vibrations of MRE sandwiches in a nonuniform magnetic field.

7.5 Free Vibrations of MRE-based Laminated Cylindrical Shells and Panels

7.5.1 Lengthy Simply Supported Cylinders

At first, let us consider Eqs. (7.11) at $q_n = 0$. They allow to describe any type of free vibrations of a shell of an arbitrary length. We will study here vibrations of long MRE-based cylindrical shells and show the effect of a magnetic field on the long wave modes.

For free linear vibrations, the solution of Eqs. (7.11) is written as

$$\{\hat{u}_i, \psi_i, w\} = R\{U_i(\alpha_1, \alpha_2), \Psi_i(\alpha_1, \alpha_2), W(\alpha_1, \alpha_2)\} \exp(\mathrm{i}\Omega t), \tag{7.27}$$

where $\Omega = \omega + \mathrm{i}\alpha$ is the required complex natural frequency, and functions U_i, Ψ_i, W satisfying the boundary conditions (7.12) are as follows:

$$\begin{gathered} U_1 = U_1^\circ \cos\frac{\pi n \alpha_1}{L} \cos\frac{m\alpha_2}{R}, \quad U_2 = U_2^\circ \sin\frac{\pi n \alpha_1}{L} \sin\frac{m\alpha_2}{R}, \\ W = W^\circ \sin\frac{\pi n \alpha_1}{L} \cos\frac{m\alpha_2}{R}, \\ \Psi_1 = \Psi_1^\circ \cos\frac{\pi n \alpha_1}{L} \cos\frac{m\alpha_2}{R}, \quad \Psi_2 = \Psi_2^\circ \sin\frac{\pi n \alpha_1}{L} \sin\frac{m\alpha_2}{R}, \end{gathered} \tag{7.28}$$

where n is a number of semi-waves in the axial direction, m is a number of waves in the circumferential direction, and $U_i^\circ, W^\circ, \Psi_i^\circ$ are constant values.

The substitution of (7.25), (7.26) into Eqs. (7.11) yields the system of algebraic equations

$$\mathbf{A}\mathbf{X}^{\mathrm{T}} = 0, \tag{7.29}$$

where $\mathbf{X} = (U_1^\circ, U_2^\circ, W^\circ, \Psi_1^\circ, \Psi_2^\circ)$ is the five-dimensional vector, and $\mathbf{A}$ is the 5×5 matrix with the elements a_{ij}:

$$
\begin{gathered}
a_{11} = -\delta_n^2 - \frac{1-\nu}{2}m^2 - \frac{(1-\nu^2)}{d}\frac{\Omega^2}{\omega_0^2}, \quad a_{12} = \frac{1+\nu}{2}\delta_n m, \\
a_{13} = \nu\delta_n, \quad a_{14} = a_{15} = 0, \quad a_{21} = \frac{1+\nu}{2}\delta_n m, \\
a_{22} = -\frac{1-\nu}{2}\delta_n^2 - m^2 - \frac{(1-\nu^2)}{d}\frac{\Omega^2}{\omega_0^2}, \quad a_{23} = -m, \quad a_{24} = a_{25} = 0, \\
a_{31} = a_{32} = 0, \quad a_{33} = -\eta_2\delta_n(\delta_n^2 + m^2), \\
a_{34} = \eta_1\left(\delta_n^2 + \frac{1-\nu}{2}m^2\right) + \frac{q_{44}R^2\eta_3}{D}, \\
a_{35} = -\frac{\eta_1(1+\nu)}{2}\delta_n m, \quad a_{41} = a_{42} = 0, \quad a_{43} = -\eta_2 m(\delta_n^2 + m^2), \\
a_{44} = -\frac{\eta_1(1+\nu)}{2}\delta_n m, \quad a_{45} = \eta_1\left(m^2 + \frac{1-\nu}{2}\delta_n^2\right) + \frac{q_{44}R^2\eta_3}{D}, \\
a_{51} = -\frac{\nu}{1-\nu^2}\delta_n, \quad a_{52} = \frac{m}{1-\nu^2}, \\
a_{53} = \varepsilon^8 g(\delta_n^2 + m^2)^2 + \frac{1}{1-\nu^2} - \frac{\Omega^2}{\omega_0^2 d}, \\
a_{54} = -\frac{\varepsilon^8 g\eta_2}{\eta_3}\delta_n(\delta_n^2 + m^2), \quad a_{55} = \frac{\varepsilon^8 g\eta_2 m}{\eta_3}(\delta_n^2 + m^2),
\end{gathered}
\tag{7.30}
$$

where

$$
\begin{gathered}
\delta_n = \frac{\pi n}{l}, \quad l = \frac{L}{R}, \quad d = \frac{E}{E_r^{(0)}}, \quad g = \frac{\eta_3[1-(\nu_r^{(0)})^2]}{\eta_{3r}^{(0)}(1-\nu^2)}, \\
\varepsilon^8 = \frac{h_*^2\eta_{3r}^{(0)}}{12[1-(\nu_r^{(0)})^2]}, \\
\omega_0^2 = \frac{E_r^{(0)}}{\rho_0 R^2}.
\end{gathered}
\tag{7.31}
$$

Here, ε is a small parameter, ω_0 is the characteristic frequency, and $E_r^{(0)}, \nu_r^{(0)}, \eta_{3r}^{(0)}$ are the real parts for the complex Young's modulus E, Poisson's ratio ν and parameter η_3, respectively, calculated at the zeroth level of an applied magnetic field ($B = 0$ mT).

The equation

$$\det \mathbf{A} = 0 \tag{7.32}$$

serves as the existence condition of a nontrivial solution of the homogeneous system (7.26). In the general case, it is a cubic equation with respect to the required frequency parameter

$$\Lambda = \frac{(1-\nu^2)\Omega^2}{d\omega_0^2}. \tag{7.33}$$

As a particular case, we consider the axisymmetric vibrations for which

$$m = U_2^\circ = \Psi_2^\circ = 0.$$

Then, the cubic equation (7.32) degenerates into the quadratic one:

$$\Lambda^2 + \left(\delta_n^2 - 1 - \mu_1\delta_n^4 r_n\right)\Lambda - \left[(1-\nu^2)\delta_n^2 + \mu_1\delta_n^6 r_n\right] = 0, \tag{7.34}$$

where

$$\mu_1 = (1-\nu^2)\varepsilon^8 g, \quad r_n = \frac{\pi^2 + \theta K\delta_n^2}{\pi^2 + K\delta_n^2}, \quad K = \frac{\pi^2 h_*^2}{\beta}, \quad \theta = 1 - \frac{\eta_2^2}{\eta_1\eta_3}. \tag{7.35}$$

For any fixed number n, there is only one the positive root

$$\Lambda = \frac{1}{2}\left\{1 - \delta_n^2 + \mu_1 r_n\delta_n^4 + \left[(1-\delta_n^2 + \mu_1 r_n\delta_n^4)^2 + 4(1-\nu^2)\delta_n^2 + 4\mu_1 r_n\delta_n^6\right]^{1/2}\right\}. \tag{7.36}$$

If $\mu_1 \to 0$, one obtains the simple formula

$$\Lambda = 1 - \delta_n^2 + \sqrt{(1-\delta_n^2)^2 + 4(1-\nu^2)\delta_n^2} \tag{7.37}$$

corresponding to the membrane shell theory. It is seen that the natural frequencies for the membrane modes do not depend on the shear parameter K.

As $K \to 0$, Eq. (7.36) gives the frequency parameter for an isotropic shell without taking into account shears. Because a parameter θ is small, it may be concluded that the incorporation of the shear parameter K into the shell model results in the reduction of the natural frequencies for any δ_n, the influence of K on eigenfrequencies being very weak for modes with small parameter δ_n and becoming essential at large δ_n and, particularly, for modes with very large number of waves n in the axial direction (and/or for a very short cylindrical shell). We note that the influence of a magnetic field on the reduced Young's modulus E is very weak and the shear parameter K is more affected by the variation of B (Mikhasev et al, 2014). Thus, changing the induction B and, in such a way, the complex shear parameter K, we can effect slightly low-frequency modes and high-frequency ones to a greater extent.

Example 7.1. Consider a cylindrical sandwich shell assembled from two stiffen outermost and innermost sheets and a soft MRE core. The face sheets are made of the ABS-plastic SD-0170 which is treated as an elastic material with the Young's modulus $E_1 = E_3 = 1.5 \cdot 10^9$ Pa, Poison's ratio $\nu_1 = \nu_2 = 0.4$ and density $\rho_1 = \rho_3 = 1.4 \cdot 10^3$ kg/m^3. Viscoelastic properties of the MRE are as specified in Fig. 7.2, and density is $\rho_2 = 2.65 \cdot 10^3$ kg/m^3.

In Fig. 7.3, the real and imaginary parts of the reduced Young's modulus, $E_r = \Re E$, $E_i = \Im E$, are plotted as the functions of the magnetic field induction B for the sandwiches with the thickness $h_1 = h_2 = 0.5$ mm of the face sheets and different thicknesses $h_2 = 3, 5, 8, 11$ mm for the MRE core. Figure 7.4 demonstrates the behaviour of the real and imaginary parts $K_r = \Re K, K_i = \Im K$ of the parameter K versus the induction B for the same sandwiches with the thicknesses h_1, h_2 specified above. Here, the imaginary magnitudes E_i and K_i characterize the damping capability of the MRE core embedded between two elastic sheets. It is seen that the effect of a magnetic field on E_r is very weak for all thicknesses h_2 of the MRE core considered. And the function $E_i(B)$, demonstrating the visible dependence on B, is small with respect to E_r and its contribution to damping of vibrations is expected to be minor. Also, it may be concluded from Fig. 7.4: the thicker the MRE core is, the stronger the effect of an applied magnetic field on the shear parameter becomes.

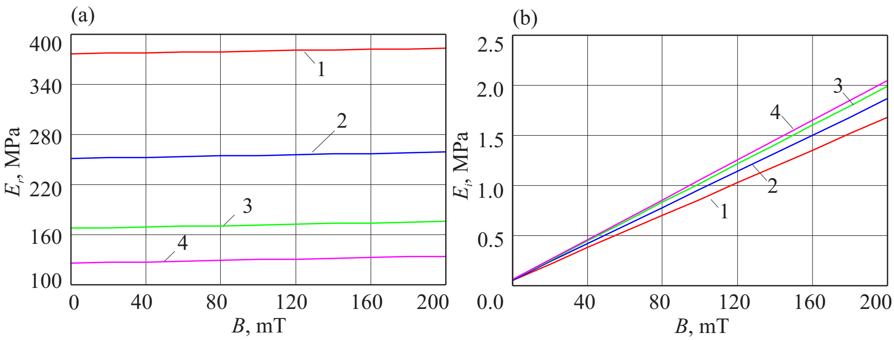

Fig. 7.3: Parameters E_r (a) and E_i (b) vs. induction B for various values of thickness $h_2 = 3(\text{line}1), 5(2); 8(3); 11(4)$ mm of the MR core

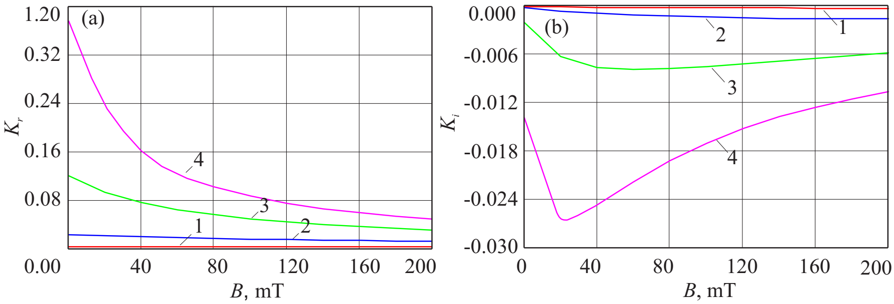

Fig. 7.4: Parameters K_r (a) and K_i (b) vs. induction B for various values of thickness $h_2 = 3(\text{line}1), 5(2); 8(3); 11(4)$ mm of the MR core

Figure 7.5 shows the influence of the induction B on the natural frequency $\omega = \Re\Omega$ and logarithmic decrement

$$D_l = \frac{\omega_i}{\sqrt{\omega^2 - \omega_i^2}} \tag{7.38}$$

corresponding to the axially symmetric modes ($m = 0$), where $\omega_i = \Im\Omega$. The calculations were performed by Eq. (7.36) for $h_2 = 11$ mm, $R = 1$ m and different values of a dimensionless parameter $\delta_n = 0.5; 1; 3; 5; 8; 11$. It is seen that the effect of a magnetic field on modes corresponding to small values of δ_n (here, for $\delta_n = 0.5; 1; 3$) is negligibly small, and it reveals itself for modes beginning approximately with $\delta_n \geq 5$, see Fig. 7.5 (b).

7.5.2 *Medium-Length Cylindrical Panels*

Consider a medium-length circular cylindrical panel with edges bounded by the curves $\alpha_1 = 0, L_1$ and generatrices $\alpha_2 = 0, L_2$, where L_1, L_2 are the panel length in the axial and circumferential directions, respectively. Physical parameters for all layers are assumed to be not dependent of coordinates α_1, α_2. To analyse free low-frequency vibrations, we consider Eqs. (7.18), (7.19), where $q_n = 0$.

Let all edges be simply supported and contain diaphragms.Then the natural modes with n and m semi-waves in the axial and circumferential directions are readily written down:

$$\begin{aligned} \chi &= \chi_a \exp(\mathrm{i}\Omega t) \sin\frac{\pi n \alpha_1}{L_1} \sin\frac{\pi m \alpha_2}{L_2}, \\ F &= F_a \exp(\mathrm{i}\Omega t) \sin\frac{\pi n \alpha_1}{L_1} \sin\frac{\pi m \alpha_2}{L_2}, \end{aligned} \tag{7.39}$$

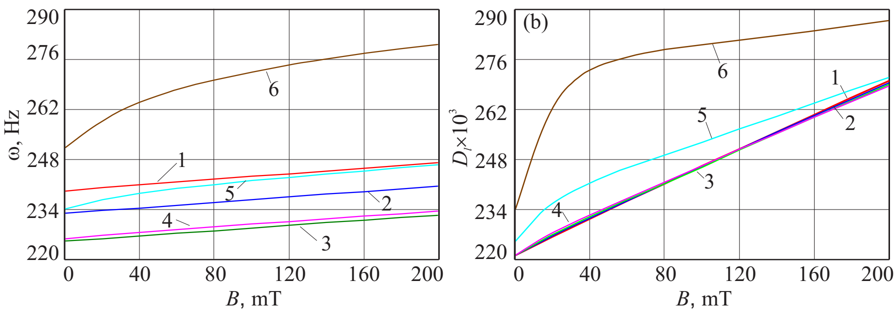

Fig. 7.5: Natural frequency ω (a) and logarithmic decrement D_l (b) vs. induction B for the axially symmetric modes and different values of a parameter $\delta_n = 0.5$ (line 1); 1 (2); 3 (3); 5 (4); 8 (5); 11 (6)

where $i = \sqrt{-1}$, and Ω is the required complex natural frequency. The substitution of (7.39) into Eqs. (7.18), (7.19) results in the following formula for eigenfrequency:

$$\Omega = \Omega_{nm} = \sqrt{\frac{E}{\rho R^2}\left\{\frac{E}{\rho R^2}\frac{[1+\theta K\triangle_{nm}]\triangle_{nm}^2}{1+K\triangle_{nm}} + \frac{n^4}{l_1^4\triangle_{nm}^2}\right\}}, \tag{7.40}$$

where

$$\eta = \frac{\pi^4\eta_3}{(1-\nu^2)}, \quad \triangle_{nm} = \left(\frac{n}{l_1}\right)^2 + \left(\frac{m}{l_2}\right)^2, \quad l_j = \frac{L_j}{R}. \tag{7.41}$$

Example 7.2. The series of calculations of the natural frequencies ω and logarithmic decrements D_l for cylindrical MRE-based sandwich panels with different opening angles $\varphi_2 = L_2/R$ and the same length $L_1 = 1$ m and radius $R = 0.5$ m were performed. The material properties of the face sheets and MRE core are the same as in Example 7.1. Thicknesses of elastic layers and viscoelastic core are $h_1 = h_3 = 0.5$ mm and $h_2 = 11$ mm, respectively. Figures from 7.6 to 7.8 show the influence of the induction B on ω and D_l corresponding to natural modes with one semi-wave ($n = 1$) in the axial direction and $m = 1;2;3;4;5$ semi-waves in the circumferential direction for the three panels with $\varphi_2 = \pi/3, \pi/2, \pi$.

As seen, for the panel with a small opening angle φ_2, the mode corresponding to the lowest eigenfrequency has the one semi-wave in both the axial and circumferential directions, and the effect of magnetic field on this mode turns out to be weak (see Fig. 7.6). For medium-length panels with a large value of φ_2 as well as for closed

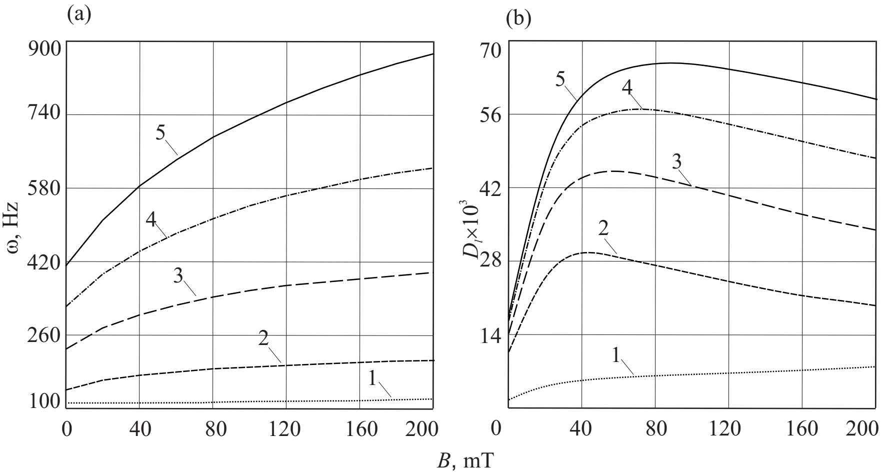

Fig. 7.6: Natural frequency ω (a) and logarithmic decrement D_l (b) for cylindrical panel with the opening angle $\varphi_2 = \pi/3$ vs. induction B for modes with one semi-wave ($n = 1$) in the axial direction and $m = 1; 2; 3; 4; 5$ semi-waves in the circumferential direction (lines 1, 2, 3, 4, 5, respectively)

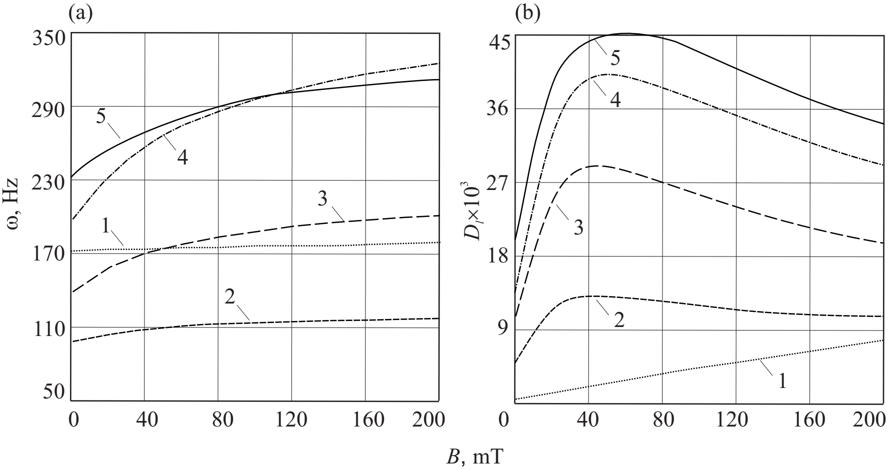

Fig. 7.7: Natural frequency ω (a) and logarithmic decrement D_l (b) for cylindrical panel with the opening angle $\varphi_2 = \pi/2$ vs. induction B for modes with one semi-wave ($n = 1$) in the axial direction and $m = 1; 2; 3; 4; 5$ semi-waves in the circumferential direction (lines 1, 2, 3, 4, 5, respectively)

cylindrical shells, the natural modes corresponding to the lowest eigenfrequencies are characterized by a number of the circumferential semi-waves of the order $m \sim h_*^{1/4}$ (Mikhasev and Tovstik, 2009); so, for $\varphi_2 = \pi$, one has $m = 4$, although for $\varphi_2 = \pi/3$, $m = 1$. As expected, the influence of a magnetic field on modes with a large number of semi-waves m are more essential than on modes with a small index of variation ι. The damping capability of the MRE core is different for panels with small and large opening angles and depends on the level of an applied magnetic field: for $\varphi_2 = \pi/3$, the logarithmic decrement of low-frequency vibrations ($m = 1$) is a slowly increasing function of B and reaches its maximum $D_l \approx 8 \cdot 10^{-3}$ at large value of $B = 200$ mT; and for $\varphi_2 = \pi/3$, the decrement for the mode with $m = 4$ has the local maximum $D_l \approx 13 \cdot 10^{-3}$ at a low level of an applied magnetic field ($B \approx 35$ mT). This conclusion is important and may be used in problems on suppression of low-frequency vibration of medium-length MRE-based cylindrical panels and shells.

7.5.3 Vibrations of Medium-Length Cylindrical Shells in Nonuniform Magnetic Field

If any layer in a sandwich or multilayered cylindrical shell is made of a polarized MRE, then the effect of an applied magnetic may be different in various parts of a shell. Indeed, an angle between the force lines of magnetic field and alignment of magnetizable particles in a polarized MRE varies from point to point in the MR

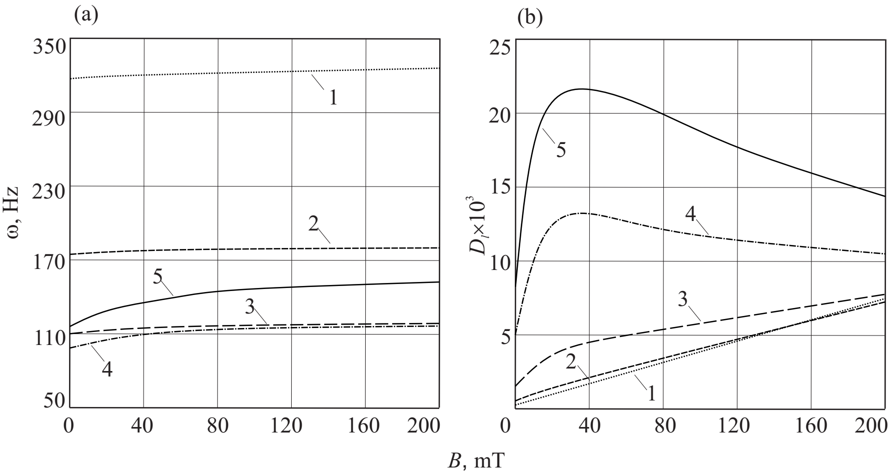

Fig. 7.8: Natural frequency ω (a) and logarithmic decrement D_l (b) for cylindrical panel with the opening angle $\varphi_2 = \pi$ vs. induction B for modes with one semi-wave ($n = 1$) in the axial direction and $m = 1; 2; 3; 4; 5$ semi-waves in the circumferential direction (lines 1, 2, 3, 4, 5, respectively)

layer (Boczkowska et al, 2012). Even if a magnetic field is uniform, the complex shear modulus of the polarized MRE turns out to be a function of curvilinear coordinates. In this case, an applied magnetic field may result in strong distortion of eigenmodes and, particularly, in localization of natural modes in the neighborhood of a generatrix where the real part of the shear modulus has a local minimum (Mikhasev et al, 2014). In this subsection, we aim to show that a nonuniform magnetic field may lead to the same effect, that is the localization of the natural modes corresponding to low-frequency vibrations of the medium-length sandwich cylindrical shell containing a homogeneous and isotropic MRE.

Let the applied magnetic field be nonuniform so that the induction $B(\varphi)$ in the MRE core is a function of an angle $\varphi = \alpha_2/R$. Then all the magneto-sensitive complex magnitudes $\nu, \eta_3, E, \theta, \beta$ appeared in Eqs. (7.19), (7.20) are functions of φ. We introduce a small parameter

$$\varepsilon^8 = \frac{h_*^2 \eta_{3r}^{(0)}}{12\left[1-\left(\nu_r^{(0)}\right)^2\right]}, \tag{7.42}$$

and assume that the shell is sufficiently thin so that h_* is a quantity of the order ~ 0.01 or less. In Eq. (7.42) and below, the superscript (0) means that an appropriate parameter is calculated at $B = 0$. Here, $\eta_{3r} = \Re\,\eta_3$, $\nu_r = \Re\,\nu$, $\nu_r^{(0)} \approx 0.4$. It is also assumed that the thickness h_2 of the MRE corer is not less then 70% from the total thickness h of the shell. Then the analysis of the the magneto-sensitive complex magnitudes for the sandwich under consideration implies the following estimations (Mikhasev et al, 2014)

$$\begin{aligned}
&\nu = \nu_r^{(0)}\left[1+\varepsilon^4\delta\nu(\varphi)\right], \quad \theta_r \sim \varepsilon^3, \quad \theta_i \sim \varepsilon^4,\\
&\eta_3 = \eta_{3r}^{(0)}\left[1+\varepsilon^2\delta\eta_3(\varphi)\right], \quad \eta_{3r}^{(0)} = \pi^{-4}\eta_r^{(0)}\left[1-(\nu_r^{(0)})^2\right],\\
&E_r = E_r^{(0)}d(\varphi) = E_r^{(0)}[1+\varepsilon d_1(\varphi)], \quad E_i/E_r^{(0)} \sim \varepsilon^4,\\
&\pi^{-2}K = \varepsilon^2\kappa(\varphi) = \varepsilon^2[\kappa_0(\varphi)+\mathrm{i}\varepsilon\kappa_1(\varphi)]
\end{aligned} \tag{7.43}$$

at $\varepsilon \to 0$. In Eqs. (7.43), $\delta\nu, \delta\eta_3$ and d_1, κ_0, κ_1 are the complex and real functions of φ, respectively, so that their absolute magnitudes are quantities of the order $O(1)$ at $\varepsilon \to 0$. In (7.43), the last estimate for K means that $\zeta_G = 3/2$ (see relation (7.15)).

The solution of Eqs. (7.19), (7.20) at $q_n = 0$ with the boundary conditions (7.24) is readily represented in the form

$$\chi = \varepsilon^{-4}R\chi^*(s,\varphi)\exp(\mathrm{i}\Omega t), \quad F = E_r^{(0)}hR^2F^*(s,\varphi)\exp(\imath\Omega t), \tag{7.44}$$

where $s = \alpha_1/R$ is a dimensionless axial co-ordinate, Ω is an unknown complex natural frequency, and χ^*, F^* are dimensionless displacement and stress functions.

The substitution of (7.44) into Eqs. (7.19), (7.20) results in the following system of differential equations with respect to χ^*, F^*:

$$\begin{aligned}
&\varepsilon^4 d(\varphi)\triangle_\varphi^2\chi^* - \delta_n^2F^* - \Lambda[1-\varepsilon^2\kappa(\varphi)\triangle_\varphi]\chi^* = 0,\\
&\varepsilon^4\triangle_\varphi^2F^* + \delta_n^2[1-\varepsilon^2\kappa(\varphi)\triangle_\varphi]\chi^* = 0,
\end{aligned} \tag{7.45}$$

where

$$\triangle_\varphi = \left(\frac{\mathrm{d}^2}{\mathrm{d}\varphi^2} + \delta_n^2\right). \tag{7.46}$$

δ_n is defined by (7.31) and

$$\Lambda = \frac{\rho R^2\Omega^2}{\varepsilon^4E_r^{(0)}}$$

is a dimensionless frequency parameter. When deriving Eqs. (7.45) from Eqs. (7.19), (7.20), we have omitted the operator $K\theta\Delta^3\chi$ because of smallness of the coefficient $K\theta$ and disregarded by very small dimensionless parameters $\varepsilon^4\delta\nu, \varepsilon^2\delta\eta_3, E_i/E_r^{(0)}$.

Let $\varphi = \varphi_0$ be a generatrix where the function $B(\varphi)$ has a local minimum. Because the storage modulus G_v' of the MRE is the increasing function of the induction B (see Fig. 7.2), then the dimensionless shear parameter κ satisfies the following conditions:

$$\kappa_0'(\varphi_0) = 0, \quad \kappa_0''(\varphi_0) < 0. \tag{7.47}$$

The problem is to find the minimum eigenvalue $\Re\Lambda$ for Eq. (7.45) satisfying the conditions

$$|\chi^*|, |F^*| \to 0 \quad \text{at} \quad |\varphi-\varphi_0| \to \infty. \tag{7.48}$$

The generatrix $\varphi = \varphi_0$ is called the weakest one. The required eigenfunctions χ^*, F^* satisfying (7.48) may be found in the form of asymptotic series (Mikhasev and Tovstik, 2009):

$$\chi^* = \sum_{j=0}^{\infty} \varepsilon^{j/2} \chi_j(\zeta) \exp\{\mathrm{i}(\varepsilon^{-1/2} p\zeta + 1/2 b\zeta^2)\},$$
$$F^* = \sum_{j=0}^{\infty} \varepsilon^{j/2} F_j(\zeta) \exp\{\mathrm{i}(\varepsilon^{-1/2} p\zeta + 1/2 b\zeta^2)\}, \tag{7.49}$$

$$\Lambda = \Lambda_0 + \varepsilon \Lambda_1 + \ldots,, \tag{7.50}$$

where $\zeta = \varepsilon^{-1/2}(\varphi - \varphi_0)$, p is the real wave parameter, b is the complex number with a positive imaginary part ($\Im\, b > 0$), and χ_j, F_j are polynomials in ζ. Here the parameter b characterizes the width of an area where more intensive vibrations occur.

The substitution of (7.49), (7.50) into Eqs. (7.45) generates the sequence of algebraic equations with respect to unknown χ_j, F_j, Λ_j. The stepwise consideration of these equations (see the details of this procedure in Tovstik and Smirnov, 2001; Mikhasev and Tovstik, 2009) results in the following formulae:

$$F_0 = -\delta_n^2 p^{-4}[1 + p^2\kappa_0(\varphi_0)]\chi_0,$$

$$\lambda_r = \Re\Lambda = f^{1/2} + \frac{\varepsilon}{2f^{1/2}}\left[\frac{(1+2m)p^3\sqrt{-f_{pp}\kappa_0''(\varphi_0)}}{2[1+p^2\kappa_0(\varphi_0)]} + d_1(\varphi_0)p^4\right] + O(\varepsilon^2), \tag{7.51}$$
$$\lambda_i = \Im\Lambda = -\frac{\varepsilon f^{1/2}\kappa_1(\varphi_0)p^2}{2[1+\kappa_0(\varphi_0)p^2]} + O(\varepsilon^2), \quad b = \frac{\mathrm{i}p^3}{1+p^2\kappa_0(\varphi_0)}\sqrt{-\frac{\kappa_0''(\varphi_0)}{f_{pp}}},$$

where

$$f(p,\varphi_0;n) = \frac{\delta_n^4}{p^4} + \frac{p^4}{1+\kappa_0(\varphi_0)p^2}, \tag{7.52}$$

and the wave number p is determined from the equation

$$\delta_n^{-4}\kappa_0(\varphi_0)p^{10} + 2p^8 - 2\kappa_0^2(\varphi_0)p^4 - 4\kappa_0(\varphi_0)p^2 - 2 = 0. \tag{7.53}$$

In Eq. (7.51), m is a nonnegative integer number, $\chi_0(\zeta)$ is the Hermitian polynomial of the mth degree, $(\ldots)'$ means differentiation with respect to φ_0, the subscript p denotes the partial derivatives of f with respect to p. For the mode corresponding to the lowest frequencies, one needs to assume $m = 0$, and $\chi_0 \equiv 1$.

The magnitude

$$\kappa_0''(\varphi_0) = \frac{B''(\varphi_0)}{\pi^2\varepsilon^2}\left.\frac{\mathrm{d}K_r}{\mathrm{d}B}\right|_{B=B(\varphi_0)} \tag{7.54}$$

depends on the rate of inhomogeneity of an applied magnetic field. The derivative $\mathrm{d}K_r/\mathrm{d}B$ is calculated using the data presented in Fig. 7.4 (a). As seen form Eq. (7.51), it influences on both the correction for the natural frequency and the parameter b, while the parameter $\kappa_1(\varphi_0)$ defines the damping ratio of vibrations localized near the generatrix $\varphi = \varphi_0$ with the lowest level of the applied magnetic field.

The following example illustrates the effect of a nonuniform magnetic field on the lowest natural frequencies and modes.

Example 7.3. Let the MRE-based sandwich cylindrical shell of the length $L = 1.5$ m and radius $R = 1$ m be in the nonuniform magnetic field. The mechanical properties and thicknesses of the face sheets and MRE core are the same as in Example 7.2. In the domain occupied by the core, the magnetic induction is assumed to be the function

$$B(\varphi) = B_0\left[1 - \xi \exp(-c\varphi^2)\right], \tag{7.55}$$

where $B_0 > 0$, $0 < \xi \leq 1$, $c > 0$. Then the weakest generatrix is the line $\varphi = \varphi_0 \equiv 0$.

Table 7.1 shows the behaviour of parameters p, λ_{r0}, λ_r, λ_i, $\Im b$, D_l with increasing the induction (parameter B_0) and constant parameters c, ξ characterizing the rate of the magnetic field inhomogeneity. Here, $\lambda_{r0} = \sqrt{f(p,0;1)}$ gives the zeroth approximation for the eigenvalue Λ. Then $\Omega_0 = \sqrt{\varepsilon^4 E_r^{(0)} \lambda_{r0}/(\rho R^2)}$ is the lowest natural frequency for the shell placed in the uniform magnetic field of the induction $B = B_0(1-\xi)$ mT. It may be seen that increasing the magnetic field with fixed parameters c, ξ (defining the rate of inhomogeneity of magnetic field) results in increasing all parameters except the wave parameter p which shows slight decreasing. As expected, the parameter $\Im b$, damping ratio λ_i and logarithmic decrement D_l are monotonically increasing functions of the induction.

Table 7.2 demonstrates the influence of a parameter c on p, λ_{r0}, λ_r, λ_i, $\Im b$, D_l at the fixed value of $B_0 = 80$ mT. A parameter c specifies the rate of inhomogeneity of the applied magnetic field. As seen, it does not effect on the wave parameter p and zeroth approximation λ_{r0} of the eigenvalue. But it essentially affects the parameter $\Im b$, correction Λ_1 and the frequency parameter λ_r in the end. As opposed to the data from Table 7.1, the damping ratio λ_i and logarithmic decrement D_l are monotonically decreasing functions of c.

The above examples allow concluding that a nonuniform magnetic field may essentially disturb the low-frequency modes in thin medium-length sandwich cylinders containing a MRE core. In particular, a magnetic field not uniformly distributed in

Table 7.1: Parameters p, λ_{r0}, λ_r, λ_i, $\Im b$, D_l vs. induction B_0 for the MRE shell in nonuniform magnetic field with parameters $\xi = 0.9$, $c = 2$

B_0, mT	p	λ_{r0}	λ_r	λ_i	$\Im b$	D_l
20	1.509	2.799	3.446	0.0114	0.197	0.0208
40	1.506	2.808	3.657	0.0126	0.262	0.0216
80	1.500	2.823	3.893	0.0143	0.331	0.0230
100	1.497	2.830	3.968	0.0148	0.351	0.0234
200	1.488	2.855	4.173	0.0159	0.394	0.0239

Table 7.2: Parameters p, λ_{r0}, λ_r , λ_i, $\Im b$, D_l vs. parameter c for the MRE shell in nonuniform magnetic field with parameters $B_0 = 80$ mT, $\xi = 0.9$

c	p	λ_{r0}	λ_r	λ_i	$\Im b$	D_l
0.5	1.500	2.823	3.409	0.0163	0.165	0.0301
1	1.500	2.823	3.617	0.0153	0.234	0.0267
2	1.500	2.823	3.893	0.0143	0.331	0.0230
3	1.500	2.823	4.091	0.0136	0.405	0.0208
4	1.500	2.823	4.250	0.0131	0.468	0.0193

the circumferential direction can result in strong localization of modes in the shell areas where the effect of a magnetic field is weak.

7.6 Forced Vibrations

In this section, we consider forced vibrations of a thin medium-length sandwich cylindrical panel containing the MRE-core under the external harmonic force

$$q_n = Q^+(\alpha_1,\alpha_2)\exp(\mathrm{i}\omega_e t) + Q^-(\alpha_1,\alpha_2)\exp(-\mathrm{i}\omega_e t), \tag{7.56}$$

where $0 < \omega_e$ is the frequency of excitation, and $Q^{\pm}(\alpha_1,\alpha_2)$ are complex functions of the curvilinear coordinates α_1,α_2.

Let all the edges $\alpha_1 = 0, L_1$, $\alpha_2 = 0, L_2$ be simply supported and have diaphragms preventing the edge shears, see Eqs. (7.24). Then the solution of the governing equations (7.19) may be represented in the form:

$$\begin{aligned} \chi(\alpha_1,\alpha_2,t) &= \sum_{n=1}^{\infty}\sum_{m=1}^{\infty} \sin\frac{\pi n\alpha_1}{L_1}\,\sin\frac{\pi m\alpha_2}{L_2}\chi_{nm}(t), \\ F(\alpha_1,\alpha_2,t) &= \sum_{n=1}^{\infty}\sum_{m=1}^{\infty} \sin\frac{\pi n\alpha_1}{L_1}\,\sin\frac{\pi m\alpha_2}{L_2} f_{nm}(t), \end{aligned} \tag{7.57}$$

Let us expend the functions $Q^{\pm}$ into the double Fourier series

$$Q^{\pm}(\alpha_1,\alpha_2) = \sum_{n=1}^{\infty}\sum_{m=1}^{\infty} q^{\pm}_{nm}\sin\frac{\pi n\alpha_1}{L_1}\,\sin\frac{\pi m\alpha_2}{L_2}, \tag{7.58}$$

where

$$q^{\pm}_{nm} = \frac{4}{L_1L_2}\int_0^{L_1}\int_0^{L_2} Q^{\pm}(\alpha_1,\alpha_2)\sin\frac{\pi n\alpha_1}{L_1}\,\sin\frac{\pi m\alpha_2}{L_2}\,\mathrm{d}\alpha_1\mathrm{d}\alpha_2. \tag{7.59}$$

The substitution of Eqs. (7.56)-(7.58) into Eqs. (7.19) leads to the sequence of differential equations

$$\ddot{q}^{\pm}_{nm} + \Omega^2_{nm} q^{\pm}_{nm} = \hat{q}^{\pm}_{nm} \mathrm{e}^{\pm \mathrm{i}\omega_e t}, \quad (n = 1,2,\ldots; m = 1,2,\ldots) \tag{7.60}$$

where Ω_{nm} are the complex natural frequencies defined by (7.40), and

$$\hat{q}^{\pm}_{nm} = \frac{q^{\pm}_{nm}}{\rho h(1 + K\triangle_{nm})} \tag{7.61}$$

are the complex magnitudes depending on the complex shear parameter K introduced by Eq. (7.35).

The partial solution of Eq. (7.60) reads

$$q^{\pm}_{p} = \frac{\hat{q}^{\pm}_{nm}}{\Omega^2_{nm} - \omega_e^2} \mathrm{e}^{\pm \mathrm{i}\omega_e t}. \tag{7.62}$$

Then the general solution of Eqs. (7.19) is

$$\chi = \chi_g + \chi_p,$$

$$\begin{aligned} \chi_g &= \sum_{n=1}^{\infty}\sum_{m=1}^{\infty} \left(c^{+}_{nm} \mathrm{e}^{\mathrm{i}\Omega_{nm} t} + c^{-}_{nm} \mathrm{e}^{-\mathrm{i}\Omega_{nm} t} \right) \sin\frac{\pi n \alpha_1}{L_1} \sin\frac{\pi m \alpha_2}{L_2}, \\ \chi_p &= \sum_{n=1}^{\infty}\sum_{m=1}^{\infty} \left(\frac{\hat{q}^{+}_{nm} \mathrm{e}^{\mathrm{i}\omega_e t} + \hat{q}^{-}_{nm} \mathrm{e}^{-\mathrm{i}\omega_e t}}{\Omega^2_{nm} - \omega_e^2} \right) \sin\frac{\pi n \alpha_1}{L_1} \sin\frac{\pi m \alpha_2}{L_2}, \end{aligned} \tag{7.63}$$

where $c^{\pm}_{nm}$ are arbitrary complex constants which are determined from the initial conditions. If $\omega_e = \Re\Omega_{nm}$ for any fixed n,m, then one has resonance vibrations by the mode with numbers n,m. As Ω_{nm} is complex, the amplitude of resonance vibrations is always a bounded magnitude.

Example 7.4. Consider a MRE sandwich with the opening angle $\varphi_2 = \pi$ and thickness $h_2 = 11$mm of the MRE core. Other geometrical and physical properties are as specified in Example 7.2. The sandwich is assumed to be motionless at $t \le 0$ so that

$$\chi|_{t=0} = \dot{\chi}|_{t=0} = 0. \tag{7.64}$$

Let the external force be the pulsing hydrostatic pressure $q_n = q_a \sin\omega_e t$ (here, $Q^{\pm} = \mp 1/2\mathrm{i}\, q_a$) which will excite vibrations in the MRE sandwich at $t > 0$. On account of the linearity of equations and nil initial conditions, the amplitude q_a is not specified here. Figure 7.9 shows the scaled maximum amplitude A of forced vibrations for $\omega_e = 40$ Hz and different values of the magnetic field induction $B = 0(\mathrm{a}), 40(\mathrm{b}), 200(\mathrm{c})$ mT applied at $t = 0$. In all cases, the double infinite series in (7.63) were replaced by double finite series with 20 terms in each series. As seen, the applied external harmonic force excites the intensive vibrations in the form of the superposition of natural modes and forced vibrations. Due to viscosity of the MRE

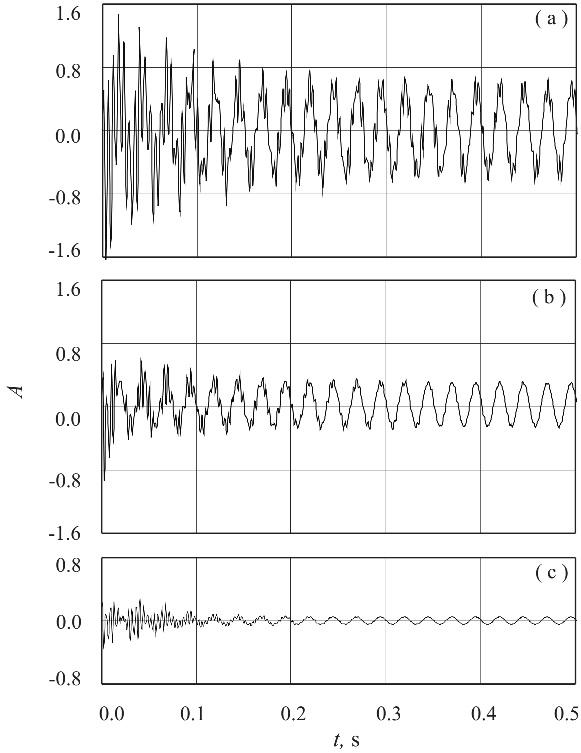

Fig. 7.9 Scaled maximum amplitude A of forced vibrations of MRE sandwich vs. time t(s) for different values of induction B of magnetic field applied at $t = 0$: (a) - $B = 0$ mT, (b) - $B = 40$ mT, (c) - $B = 200$ mT

core, the excited natural modes attenuates during time with damping rate depending on the intensity of applied magnetic field, the higher the level of magnetic field is, the faster decaying of natural modes becomes. Suppression of forced vibrations of the frequency $\omega_e = 40$ Hz are also influenced by the induction B. However, the nature of this vibration damping is another: increasing the magnetic field induction leads to increasing eigenfrequencies for all modes, see Fig. 7.6 (b), and results in fast decreasing the amplitudes

$$\sum_{n=1}^{\infty}\sum_{m=1}^{\infty}\hat{q}_{nm}^{\pm}(|\Omega_{nm}^2| - \omega_e^2)^{-1}$$

in the end.

In the above calculations, the magnetic field and external force were applied at once. Consider the next example illustrating the response of the MRE sandwich to the magnetic field and external force applied at different points of time.

Example 7.5. Let the initial conditions be again given by (7.64), the harmonic force $q_n = q_a \sin\omega_e t$ is applied at $t = 0$, while the magnetic field of the induction $B = 200$ mT is supplied at $t = t_k > 0$. The frequency ω_e is the same as in Example 7.4. Let $\chi^{(1)}(\alpha_1, \alpha_2, t)$ be the solution of the initial value problem (7.19), (7.64) at the interval

$0 \le t \le t_k$. Consider the following initial conditions:

$$\chi|_{t=t_k} = \chi^{(1)}(\alpha_1,\alpha_2,t_k), \quad \dot{\chi}|_{t=t_k} = \dot{\chi}^{(1)}(\alpha_1,\alpha_2,t_k). \tag{7.65}$$

The solution of the initial value problem (7.19), (7.65) at $t \ge t_k$ and $B = 200$ mT is designated by $\chi^{(2)}(\alpha_1,\alpha_2,t)$. After applying the magnetic field at $t = t_k$ the viscoelastic properties of the sandwich are changed instantaneously. So, to use formula (7.63) at $t \ge t_k$, one needs to recalculate at first all natural frequencies for the sandwich and then complex magnitudes (7.61) at $B = 200$ mT. The parametric impact caused by the suddenly applied magnetic field is not taking into account here (see an example in Korobko et al, 2012).

Figure 7.10 shows the response of the MRE sandwich in two cases, when $t = t_1 = 0.1$s (a) and $t = t_2 = 0.2$s (b). The drawn lines at $0 \le t < t_k$ represent the scaled maximum amplitudes for the displacement functions $\chi^{(1)}$ without a magnetic field, while the lines for $t \ge t_k$ correspond to $\chi^{(2)}$ calculated at $B = 200$ mT. In the both cases, the application of a magnetic field results in the rapid and effective suppression of vibrations consisting of the superposition of the natural modes and the essential reduction of the forced vibrations as well. The comparison of Figs. 7.10(a) and (b) allows to conclude: for the effective suppression of excited natural modes the magnetic field should be supplied as soon as possible.

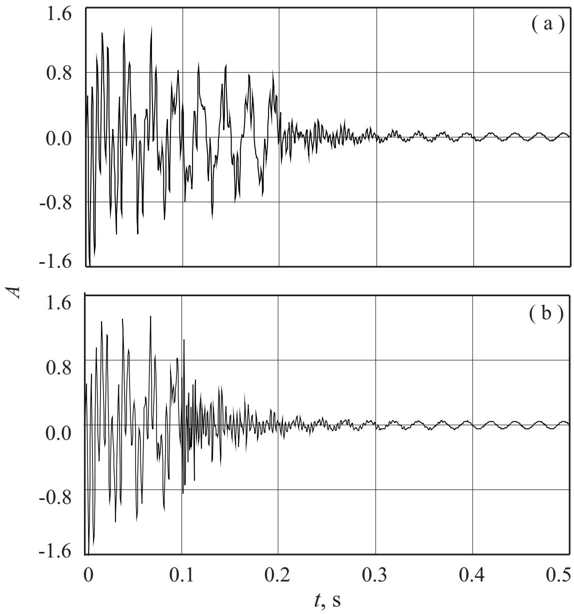

Fig. 7.10 Response of MRE sandwich to harmonic force and magnetic field applied at different points of time t_k: (a) - $t_k = 0.1$ s, (b) - $t_k = 0.2$ s

7.7 Conclusions

The equivalent single layer theory based on the assumptions of the generalized kinematic hypotheses of Timoshenko for laminated shells was used to study both free and forced vibrations of sandwich cylindrical shells and panels containing MRE cores under various levels of applied magnetic fields. To analyze free vibrations of length cylindrical shells, the system of five differential equations accounting transverse shears and written in terms of generalized displacements was assumed as the system of governing equations. To predict free and forced vibrations of medium-length cylindrical shells and panels, the simplified equations with respect to the displacement and force functions were used.

Assuming the boundary conditions of simply supported edges with diaphragms, formulae for complex natural frequencies for both length and medium-length cylindrical shells and panels were obtained. The analysis of performed calculations for a long sandwich cylinder has shown that the influence of an applied magnetic field on the natural frequencies corresponding to modes with small numbers of waves in the axial and circumferential directions is weak. In particular, the damping effect of the MRE core turns out to be small for axially symmetric modes with number of waves in the axial direction varying from one to four. The analysis of the natural modes for medium-length cylindrical panels has revealed that the damping capability of the MRE core is different for panels with small and large opening angles and strongly depends on the level of an applied magnetic field. It has been also displayed that a nonuniform magnetic field may result in the localization of the low-frequency natural modes in the medium-length circular sandwich cylinder containing the MRE core, the localization taking place in the neighborhood of the generatrix at which the real part of the reduced shear modulus has a local minimum.

The special attention has been given to the analysis of forced vibrations of the MRE-based sandwich cylindrical panels subjected to the external pulsing pressure. The initial conditions for displacement and velocities were assumed to be zero. A solution of the initial nonhomogeneous boundary-value problem has been found in the form of series by the natural modes of the shell and represented by the sum of the general solution of homogeneous equations and the partial solution of nonhomogeneous equations. In the first example, the external force and magnetic field were applied simultaneously. Due to controllable viscosity of the MRE core, the excited natural modes corresponding to the general solution of the homogeneous equations attenuated with the damping rate depending on the induction of an applied magnetic field. The attenuation of amplitudes of forced vibrations given by the partial solution of the nonhomogeneous equations is also governed by the magnetic field, however the nature of this damping is another: it is explained by increasing the storage modulus of the MRE core under increasing the magnetic field induction. In the second example, the magnetic fields were applied at different points of time t_k. The solutions found at the segment $0 \le t \le t_k$ and calculated for $t = t_k$ were assumed then as the initial conditions for another problem considered for $t \ge t_k$. At that, to predict the response of the sandwich at $t \ge t_k$, the natural modes were recalculated taking into account the new viscoelastic properties acquired by the shell after switching the magnetic field on. The comparative analysis of performed calculations has shown that for the effective suppression of excited vibrations the magnetic field should be supplied as soon as possible, the damping rate depending on the level of the applied magnetic field.

Acknowledgements The research leading to these results has received support from the People Programme (Marie Curie Actions) of the European Union's Seventh Framework Programme FP7/2007-2013/under REA grant agreement PIRSES-GA-2013-610547-TAMER. The first and second authors also acknowledge the support from both the ERASMUS+ Programme (Higher Education Mobility Agreement- 2016-2017 between Keele University, UK, and Belarusian State University, Belarus) and State Program of Scientific Investigations in Belarus "Physical Materials Science, New Materials and Technologies" (Assignment N 3.4.01).

References

Aguib S, Noura A, Zahloul H, Bossis G, Chevalier Y, Lançon P (2014) Dynamic behavior analysis of a magnetorheological elastomer sandwich plate. Int J Mech Sc 87:118–136

Banerjee JR, Cheung CW, Morishima R, Perera M, Njuguna J (2007) Free vibration of a three-layered sandwich beam using the dynamic stiffness method and experiment. Int J Solids Struct 44(22):7543 – 7563

Boczkowska A, Awietjan SF, Pietrzko S, Kurzydlowski KJ (2012) Mechanical properties of magnetorheological elastomers under shear deformation. Composites: Part B 43:636–640

Bolotin VV, Novichkov YN (1980) Mechanics of Multilayer Structures (in Russ.). Mashinostroenie, Moscow

Carrera E (1999) Multilayered shell theories accounting for layerwise mixed description. Part 1: Governing equations. AIAA J 37(9):1107–1116

Carrera E (2002) Theories and finite elements for multilayered, anisotropic, composite plates and shells. Arch Comput Methods Engng 9(2):87–140

Carrera E (2003) Theories and finite elements for multilayered plates and shells: a unified compact formulation with numerical assessment and benchmarking. Arch Comput Methods Engng 10:215–296

Davis LC (1999) Model of magnetorheological elastomers. J Appl Phys 85:3348–3351

Donnell LH (1976) Beams, Plates and Shells. McGraw-Hill Inc, New York

Ferreira AJM, Carrera E, Cinefra M, Roque CMC (2011) Analysis of laminated doubly-curved shells by a layerwise theory and radial basis functions collocation, accounting for through-the-thickness deformations. Comput Mech 48(1):13–25

Gibson RF (2010) A review of recent research on mechanics of multifunctional composite materials and structures. Comp Struct 92(12):2793–2810

Ginder GM (1996) Rheology controlled by magnetic fields. Encycl Appl Phys 16:487–503

Ginder GM, Schlotter WF, Nichhols ME (2001) Magnetorheological elastomers in tunable vibration absorbers. In: Proc. SPIE. **3985**, pp 418–424

Gol'denveiser AL (1961) Theory of Thin Elastic Shells. International Series of Monograph in Aeronautics and Astronautics, Pergamon Press, New York

Grigolyuk EI, Kulikov GM (1988a) General direction of development of the theory of multilayered shells. Mechanics of Composite Materials 24(2):231–241

Grigolyuk EI, Kulikov GM (1988b) Multilayer Reinforced Shells. Calculation of Pneumatic Tires (in Russ.). Mashinostroenie, Moscow

Howson WP, Zare A (2005) Exact dynamic stiffness matrix for flexural vibration of three-layered sandwich beams. J Sound Vibr 282(3):753–767

Hsu TM, Wang JTS (2005) A theory of laminated cylindrical shells consisting of layers of orthotropic laminae. AIAA J 8(12):2141–2146
Jolly MR, Bender JW, Carlson DJ (1999) Properties and applications of comercial magnetorheological fluids. J Intell Mater Syst Struct 10:5–13
Koiter WT (1966) On the nonlinear theory of thin elastic shells. Proc Koninkl Acad Westenschap B 69:1–54
Korobko EV, Mikhasev GI, Novikova ZA, Zurauski MA (2012) On damping vibrations of three-layered beam containing magnetorheological elastomer. J Intell Mater Syst Struct 23(9):1019–1023
Lara-Prieto V, Parkin R, Jackson M, Silberschmidt V, Kesy Z (2010) Vibration characteristics of mr cantilever sandwich beams: experimental study. Smart Mater Struct 19(9):015,005
Mikhasev GI, G BM (2017) Effect of edge shears and diaphragms on buckling of thin laminated medium-length cylindrical shells with low effective shear modulus under external pressure. Acta Mech 228(6):2119–2140
Mikhasev GI, Tovstik PE (2009) Localized Vibrations and Waves in Thin Shells. Asymptotic Methods (in Russ.). FIZMATLIT, Moscow
Mikhasev GI, Seeger F, Gabbert U (2001) Comparison of analytical and numerical methods for the analysis of buckling and vibrations of composite shell structures. In: Proc. of "5th Magdeburg Days of Mechanical Engineering", Otto-von-Guericke-University Magdeburg, Logos, Berlin, pp 175–183
Mikhasev GI, Botogova MG, Korobko EV (2011a) Theory of thin adaptive laminated shells based on magnetorheological materials and its application in problems on vibration suppression. In: Altenbach H, Eremeyev V (eds) Shell-like Structures, Springer, Heidelberg, Advanced Structured Materials, vol 15, pp 727–750
Mikhasev GI, Mlechka I, Altenbach H (2011b) Soft suppression of traveling localized vibrations in medium-length thin sandwich-like cylindrical shells containing magnetorheological layers via nonstationary magnetic field. In: Awrejcewicz J (ed) Dynamical Systems: Theoretical and Experimental Analysis, Springer, Switzerland, Springer Proceedings in Mathematics & Statistics, vol 182, pp 241–260
Mikhasev GI, Altenbach H, Korchevskaya EA (2014) On the influence of the magnetic field on the eigenmodes of thin lami-nated cylindrical shells containing magnetorheological elastomer. Compos Struct 113:186–196
Mushtari K, Galimov K (1961) Nonlinear Theory of Thin Elastic Shells. NSF-NASA, Washington
Qatu MS (2004) Vibration of laminated shells and plates. Elsevier, San Diego
Qatu MS, Sullivan RW, Wang W (2010) Recent research advances on the dynamic analysis of composite shells: 2000-2009. Comp Struct 93(1):14–31
Reddy JN (2003) Mechanics of Laminated Composite Plates and Shells: Theory and Analysis. CRC Press, Boca Raton
Sun Q, Zhou JX, Zhang L (2003) An adaptive beam model and dynamic characteristics of magnetorheological materials. J Sound Vibr 261:465–481
Toorani MH, Lakis AA (2000) General equations of anisotropic plates and shells including transverse shear deformations, rotary inertia and initial curvature effects. J Sound Vibr 237(4):561–615
Tovstik PE, Smirnov AL (2001) Asymptotic Metods in the Buckling Theory of Elastic Shells. World Scientific, Singapore
White JL, Choi DD (2005) Polyolefins: Processing, Structure, Development, and Properties. Carl Hanser Verlag, Munich
Wlassow WS (1958) Allgemeine Schalentheorie und ihre Anwendung in der Technik. Akademie-Verlag, Berlin
Yeh JY (2011) Vibration and damping analysis of orthotropic cylindrical shells with electrorheological core layer. Aerospace Sc Techn 15(4):293–303
Yeh JY (2013) Vibration analysis of sandwich rectangular plates with magnetorheological elastomer damping treatment. Smart Mater Struct 22(3):035,010
Yeh JY (2014) Vibration characteristics analysis of orthotropic rectangular sandwich plate with magnetorheological elastomer. Proc Engng 79:378–385

Ying ZG, Ni YQ, Ye SQ (2014) Stochastic micro-vibration suppression of a sandwich plate using a magneto-rheological visco-elastomer core. Smart Mater Struct 23(2):025,019
Zhou GY, Wang Q (2005) Magnetorheological elastomer-based smart sandwich beams with non-conductive skins. Smart Mater Struct 14(5):1001–1009
Zhou GY, Wang Q (2006) Use of magnetorheological elastomer in an adaptive sandwich beam with conductive skins. Part II: Dynamic properties. International Journal of Solids and Structures 43(17):5403–5420